INTESTINAL CAPILLARIES

I. Permeability to Peroxidase and Ferritin

F. CLEMENTI and G. E. PALADE

From The Rockefeller University, New York 10021. Dr. Clementi's present address is Università degli Studi, Istituto di Farmacologia e di Terapia, Milan, Italy

ABSTRACT

Horseradish peroxidase (mol. diam. $\simeq$50 A) and ferritin (mol. diam. $\simeq$110 A) were used as probe molecules for the small and large pore system, respectively, in blood capillaries of the intestinal mucosa of the mouse. Peroxidase distribution was followed in time, after intravenous injection, by applying the Graham-Karnovsky histochemical procedure to aldehyde-fixed specimens. The tracer was found to leave the plasma rapidly and to reach the pericapillary spaces 1 min post injection. Between 1 min and 1 min 30 sec, gradients of peroxidase reaction product could be demonstrated regularly around the capillaries; their highs were located opposite the fenestrated parts of the endothelium. These gradients were replaced by even distribution past 1 min 30 sec. Ferritin, followed directly by electron microscopy, appeared in the pericapillary spaces 3–4 min after i.v. injection. Like peroxidase, it initially produced transient gradients with highs opposite the fenestrated parts of the endothelium. For both tracers, there was no evidence of movement through intercellular junctions, and transport by plasmalemmal vesicles appeared less efficient than outflow through fenestrae. It is concluded that, in the blood capillaries of the in-intestinal mucosa, the diaphragms of the endothelial fenestrae contain the structural equivalents of the small pore system. The large pore system seems to be restricted to a fraction of the fenestral population which presumably consists of diaphragm-free or dia-phragm-deficient units.

INTRODUCTION

Regional differences in the permeability of blood capillaries to large, water-soluble molecules are well established in mammals (1–3). Transport kinetics from blood to lymph, and lymph/plasma concentration ratios of size-graded molecules indicate that permeability increases in the order: limb capillaries < intestine capillaries < liver sinusoids (1, 2). These differences are currently explained (1, 3, 4) by two postulates: (a) capillary walls are generally provided with two sets of pores—small and large—with equivalent diameters of ~90 A and ~500 A, respectively; (b) the frequency of large pores increases in the order mentioned, the ratio large to small pores being ~1:30,000 and ~1:340 in leg capillaries and liver sinusoids respectively.

Data available for intestinal capillaries are more limited. The diameter of their small pores is estimated at ~220 A by Mayerson et al. (2) who give the same value for the small pores of cervical capillaries. The latter have also been studied by Grotte (1) who has calculated a diam-eter of 70–90 A for the small pores. Since Grotte's treatment of the data is more comprehensive, we shall assume that the same dimensions obtain for the small pore system of intestinal capillaries.

In the estimate of Mayerson et al. (2), the large pores account for ~20% of the aggregate area of both pore systems, but the figure is questionable because it is higher than Grotte's (1) estimate for liver sinusoids (1:340 or ~9%), although protein concentration is lower in intestinal (4-5%) than in hepatic lymph (6%) (see reference 3). Based on Grotte's data (1), the ratio large pore: small pore in intestinal capillaries should be smaller than 1:340, which would correspond to less than 1 large pore/17 μ^2 of endothelial surface.

Electron microscopical studies have shown that there are also regional differences in the construction of blood capillaries (5), but permeability characteristics and structural features have not yet been correlated because until recently the structural equivalents of the two pore systems were unknown. Recent work using ferritin (diam.

Peroxidase and ferritin were used as probe molecules to identify the structural equivalents of the small and large pores respectively, and to find out the relationship of these equivalents to the structural features just mentioned.

EXPERIMENTAL

Materials

The experiments were carried out in adult (25-30 g) male mice of the RU strain.

Electrophoretically purified horseradish peroxidase was obtained from Worthington Biochem. Corp. (Freehold, N.J.) as a solution of 0.8-0.6 mg/ml. Horse spleen ferritin, obtained as a 10% cadmium-free solution from Pentex Corp. (Kankakee, Illinois), was further purified by 36-hr dialysis against 0.1 M EDTA[1] in 0.07 M phosphate buffer (pH 7.2), followed

TABLE I

Number of Mice Used for Each Time Point after Intravenous Injection of Tracer

(Specimens examined by electron microscopy in all cases)

Tracer	Time points															Total No. of samples
	min 1	min 1¼	min 1½	min 1¾	min 2	min 3	min 4	min 5	min 8	min 10	min 15	min 20	min 30	hr 1	hr 24	
Horseradish peroxidase	6	4	3	1	8			8		6	1			2	1	41
Ferritin				1		4	4	5	3	2	5	1	2	1	1	30

≈110 A) as a probe molecule for large pores has shown that the function of the latter is carried out in muscle capillaries by plasmalemmal vesicles (6). In the meanwhile, Karnovsky (7) has brought forward evidence which, in his interpretation, identifies the small pore system with the intercellular spaces of the endothelium in the capillaries of the myocardium and skeletal muscles. In his experiments, the probe molecule used was horseradish peroxidase (diam. ≈50 A).

The present investigation concerns the blood capillaries of the intestinal mucosa which are known to have the typical organization of visceral capillaries, i.e., they have a discontinuous adventitia, a continuous basement membrane, and a discontinuous endothelium provided with apertured fenestrae, in addition to plasmalemmal vesicles and intercellular junctions (5, 8-12).

by 48-hr dialysis against phosphate buffer alone (13); it was subsequently concentrated up to three times by sedimentation (at 105,000 g for 12 hr in a Spinco 40-3 rotor), followed by resuspension in saline.

Methods

TRACER EXPERIMENTS AND TISSUE PROCESSING

Each mouse received, by injection into a tail vein, 0.3 ml of saline alone or containing either 250-260 μg of peroxidase, or 90 mg of ferritin. At the doses of peroxidase and ferritin used, no signs of acute or delayed toxicity were observed. In contradistinction with the situation in other species, peroxidase does

---

[1] Abbreviations used: peroxidase, horseradish peroxidase; EDTA, disodium ethylenediamine-tetraacetate; Tris, Tris (hydroxymethyl)aminomethane.

not induce degranulation of mast cells and does not release histamine in mice (7).

Tissue specimens were taken under ether anesthesia at different times after injecting the tracer (see Table I), and were fixed in 4% formaldehyde and 5% glutaraldehyde in 0.1 M phosphate buffer (pH 7.4) as recommended by Karnovsky (14).

Upon laparatomy, a loop of the small intestine was exposed and fixed by injecting the fixative into its lumen and applying it at the same time to its surface. To retain the blood plasma in the vascular lumina, the loop and its mesentery were ligated at the beginning of the injection. After a few minutes of fixation in situ, the loop was excised and immersed in the same fixative for 2 hr at ~4°. Small pieces, cut from the wall of the fixed intestine, were washed overnight in 0.1 M phosphate buffer (pH 7.4) at ~4° and subsequently sectioned into ~50-100-μ slices with a Smith-Farquhar tissue sectioner (15). These slices were incubated for 1 hr at room temperature in the Graham-Karnovsky medium (16) (0.05 M Tris-HCl buffer, pH 7.6, 10 ml, containing 0.01% H_2O_2 and 10 mg of 3-3'-diaminobenzidine tetrahydrochloride), then washed three times in distilled water, and postfixed for 2 hr in 1% OsO_4 in 0.1 M phosphate buffer (pH 7.4). The blocks were stained for 15 min at ~4° with uranyl acetate (17), then dehydrated, embedded in Epon (18), and sectioned with diamond knives on a Porter Blum MT2—or Reichert OM U2 microtome. The sections were stained with uranyl acetate and lead citrate (19) and examined in a Siemens Elmiskop I or Hitachi HU 11C electron microscope.

Specimens taken from the intestinal wall of ferritin-injected mice were processed as above, except for incubation in the peroxidase medium.

Lymph Experiments

The thoracic duct was cannulated with small polyethylene tubing, 0.7 mm external diameter (PE 10 Intramedic, Clay-Adams, Inc., New York), by the technique of Boak et al. (20), as modified by Morse et al. (21). Identification of the duct was facilitated by giving the mice 0.2 ml of olive oil by gastric intubation 2 hr before cannulation. With the cannula in place, 0.5 ml of saline was given subcutaneously, and the animals were allowed free access to water. When the lymph became clear and its flow constant (0.5-0.8 ml/hr, usually after 12-18 hr), the tracer substance was injected intravenously and lymph samples collected over chosen intervals. At the end of each interval, we collected also small amounts of blood (0.1-0.2 ml) from the venous plexus of the orbit.

Peroxidase in plasma and lymph was measured spectrophotometrically, by the method of Strauss (22), following, over 2 min at 515 mμ, the transformation of N,N-dimethyl-p-phenylenediamine into a red pigment in the presence of H_2O_2. Figures obtained for plasma were corrected for the slight peroxidase activity of plasma hemoglobin. The latter was measured spectrophotometrically at 576 mμ. The lymph has no endogenous peroxidase activity.

Lymph and plasma samples from ferritin-injected animals were cleared of cells by a low-speed centrifugation and then centrifuged at 105,000 g for 12 hr in a Spinco 40-3 rotor.[2] The pellet obtained was resuspended in water and the amount of ferritin determined spectrophotometrically at 350 mμ.

OBSERVATIONS

The capillary bed of the intestinal wall is structurally heterogeneous. The vessels of the mucosa, which are of the fenestrated or visceral type and are concentrated in the villi, represent by far the predominant component of the entire capillary bed of the organ. The vessels of the muscularis, which—like muscle capillaries—have a continuous endothelium, represent a minority component[3]; their contribution to the over-all permeability of the intestinal capillary bed is probably negligible.

Our observations concern exclusively the fenestrated capillaries of the mucosa. Within the villi, they are concentrated immediately under the epithelium, separated from it by variable, but usually small (~ 0.5 μ) distances (Fig. 1). Larger vessels are located closer to the axis of the villus.

The capillary wall consists of three successive layers or tunics (endothelium, basement membrane, and adventitia) whose organization will be briefly reviewed.

The endothelium comprises a single layer of flattened cells. Their perikarya, containing the nuclei and most cell organs (centrioles, Golgi complex, lysosomes, multivesicular bodies, endoplasmic reticulum, mitochondria, rod-shaped bodies,[4] microtubules, etc.), are usually located

---

[2] Preliminary experiments had shown that this centrifugation was sufficient to sediment practically all the ferritin of the samples.

[3] Quantitative data are not available for the mouse intestine. For the dog stomach (which has a thicker muscle layer) the distribution of blood flow is 72% through the mucosa vessels and 13 and 15% through those of the submucosa and muscularis, respectively (23).

[4] Such bodies, originally described in arterial endothelia (24) and later found in all vascular endothelia (25), appear to be much more frequent in intestinal than in muscle capillaries.

along the side facing the center of the villus (Figs. 1 and 7). The periphery of these cells is attenuated to 0.15 μ or less and characteristically provided with clustered fenestrae which usually face the epithelium (Fig. 1). Each fenestra is a circle with a diameter of 350–450 A (Fig. 4). The spacing (center-to-center) within a cluster varies from 750 to 1300 A, and grazing sections indicate that the distribution of the fenestrae is random. The fenestrated parts of the endothelium amount to $\sim\frac{1}{3}$, and the aggregate surface of the fenestrae to $\sim\frac{1}{10}$ of the surface of the layer. Around the rim of each fenestra the plasmalemma on the blood front is continuous with that on the tissue front of the cell. The rim is usually pulled into a sharp wedge by the insertion of the diaphragm, which consists of a single dense layer continuous with the outer leaflet of the plasmalemma, is of uneven thickness (20–40 A), and is often provided with a central knob of $\sim$150 A (Figs. 2 and 3). Along the rim, the thickness of the light layer of the plasmalemma is occasionally increased to 40–55 A (Fig. 2).

With the evidence available we cannot decide whether the diaphragms are truly continuous structures. In grazing sections (face views), their density is uneven, with dense streaks radiating from the central knob (Fig. 4); in normal sections (Fig. 3), they do not show interruptions, but in view of the thickness of our sections and of the

relatively low density of the diaphragms the existence of discontinuities is not excluded.

In addition to usual fenestrae, the attenuated parts of the endothelium show short cylindrical channels provided at each end with a diaphragm identical in structure to those already described (Fig. 3). Appearances suggestive of the formation of such channels by the fusion of plasmalemma vesicles with the cell membrane on both cell fronts (see reference 26) are also occasionally encountered: they take the form of channels closed on one side by a single-layered aperture and on the other by a three or five-layered diaphragm (Fig. 5).

The endothelial cells have a relatively small population of plasmalemmal vesicles usually concentrated in their thicker, nonfenestrated parts. In morphology and relationship to the plasmalemma, they are similar to those described in the endothelium of other capillaries (26), except that diaphragmed forms are more frequently seen than flask-shaped vesicles (Fig. 1).
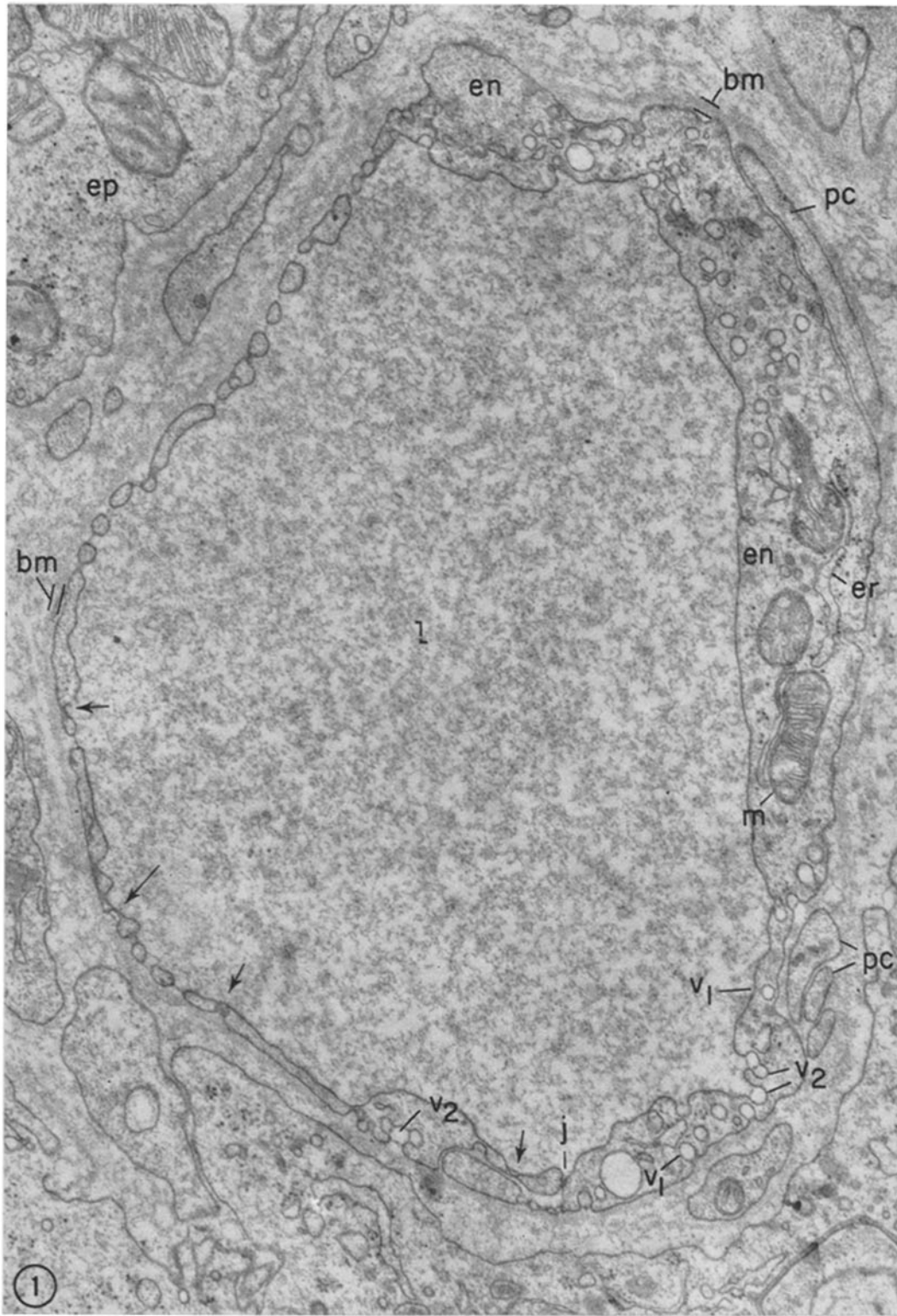
The attenuated periphery of the cells contains some mitochondria, multivesicular and rod-shaped bodies, elements of the endoplasmic reticulum, and microtubules usually in much less concentration than in perikarya.

Junctional elements are located on the frequently thickened edge of the endothelial cells and consist of one or two narrow areas in which

---

General Abbreviations

cm, plasmalemma (cell membrane)	*rbc*, red blood cell
ol, outer leaflet of the plasmalemma	*en*, endothelium
il, inner leaflet of the plasmalemma	*bm*, basement membrane
fs, fenestra	*pc*, pericyte
d, diaphragm	*ep*, epithelium of the intestinal mucosa
v, plasmalemmal vesicle	f_1, ferritin in the plasma
j, junctional element	f_2, ferritin in the pericapillary spaces
l, lumen	

FIGURE 1 Cross-section of a blood capillary in the intestinal mucosa. The endothelial layer consists of a single cell whose attenuated part faces the intestinal epithelium (*ep*) and accounts for $\sim$40% of the total endothelial surface. Its thicker part (perikaryon) contains a few mitocondria and ER cisternae and faces the center of the villus. The attenuated part is provided with numerous fenestrae closed by diaphragms; their aggregate area amounts to $\sim$5% of the endothelial surface. Images suggestive of the type of plasmalemma fusion that results in the formation of fenestrae are indicated by arrows. The thicker part of the endothelium is provided with a few flask-shaped vesicles (v_1) and many apertured vesicles (v_2) which open on both cell fronts and occur either isolated or in small clusters. The continuous basement membrane is marked *bm;* pericyte pseudopodia appear at *pc*. $\times$ 29,000.
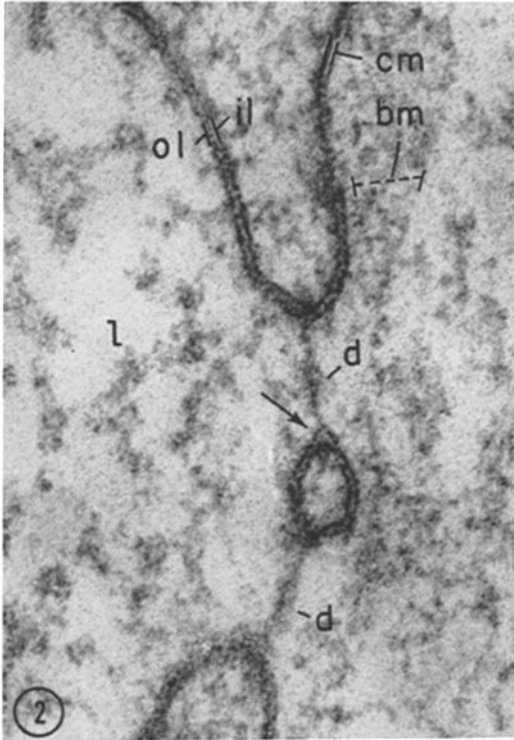
FIGURE 2 Structural details of two endothelial fenestrae. The micrograph illustrates the continuity of the diaphragms with the outer leaflet of the plasmalemma and the latter's thickened light leaflet (arrow) and sharp edge at the points of diaphragm insertion. × 335,000.

the outer leaflets of the adjacent plasmalemmae are either fused or in close apposition (Fig. 6 a; see also Fig. 12 b). Junctions with a resolvable gap (7) are rarely encountered, but junctions "short cut" by fenestrae or channels—opening in the intercellular space abluminal to the areas of membrane apposition or fusion—occur quite frequently (Fig. 6 b).

The basement membrane surrounding the intestinal capillaries is formed by a layer of fine fibrillar material, similar to that surrounding other capillaries. It encloses completely the endothelial cell and the adjacent pericytes.

The adventitia is a discontinuous, poorly outlined layer in full continuity with the pericapillary spaces. It comprises a large number of macrophages, plasmocytes, eosinophils, and a few mast cells, together with large bundles of fine fibrils (see references 27, 28) and collagen fibrils.

Peroxidase Experiments

With the method we used for fixing the intestine, the plasma was satisfactorily retained in most capillaries. From the first time point until 1 hr after the injection, the product of the peroxidase reaction filled completely the vascular lumina with a very opaque, amorphous, nearly homogeneous mass which could occasionally be resolved into packed lumps of ~200 A diameter. When the plasma was only partially retained, the reaction product appeared broken down into such lumps which usually adhered to the surface of the endothelium.

As early as 1 min or 1 min and 15 sec after the injection, some reaction product was already found in the outer layers of the capillary wall and in the pericapillary spaces. It was always localized along the fenestrated parts of the endothelium (Figs. 7 and 8) and often showed concentration gradients with their highs centered on clustered fenestrae (Figs. 7–9). Such gradients were particularly striking when the fenestrae opened into narrow interstitia in between endothelial cells and pericytes, for instance (Fig. 10). In a few cases, spotlike concentrations of reaction product were found localized outside single fenestrae (Fig. 11). Little or no reaction product was detected in the pericapillary spaces facing the thick, nonfenestrated parts of the endothelium. The luminal ends of the intercellular spaces were filled with reaction product, which penetrated only as far as the junctional element(s) (Fig. 12); the tissue end of the intercellular spaces was free, except for situations in which either a fenestra or a labeled plasmalemmal vesicle opened therein.

At this early stage, practically all plasmalemmal vesicles opening on the blood front of the endothelial cells were loaded with reaction product, but few vesicles in the cytoplasm were similarly marked (Fig. 7). Labeled vesicles were also found in small numbers on the tissue front of the endothelium, where some of them appeared to be opening and discharging (Figs. 7 and 9). Occasionally, reaction product gradients, centered on groups of such vesicles, were seen in the pericapillary spaces; they were, however, much less frequent and less evident than those related to clustered fenestrae.

After 1 min 30 sec and 2 min, the reaction product was found throughout the pericapillary spaces. The intensity of the reaction was still lower than in capillary lumina, but the density
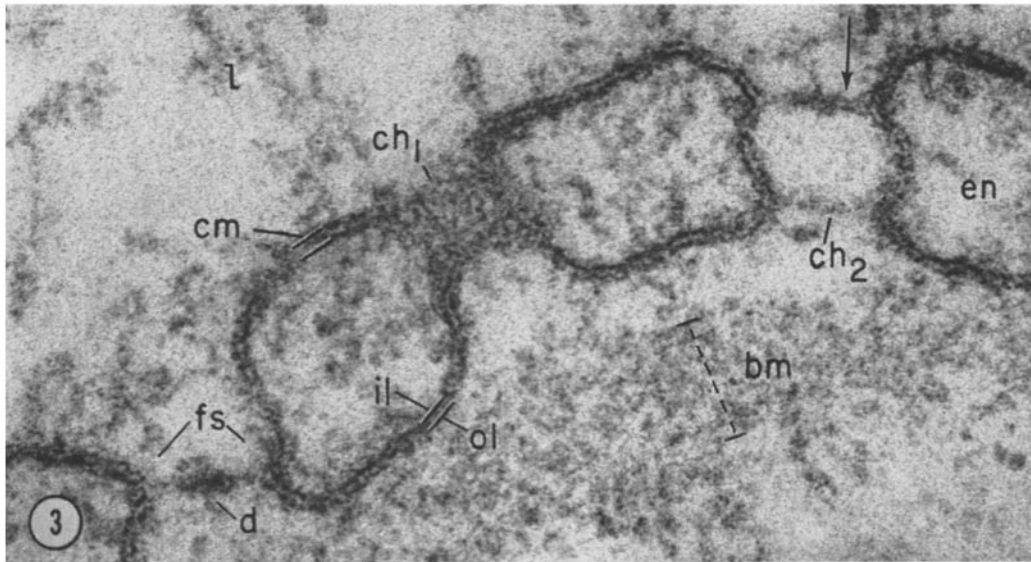
FIGURE 3 Attenuated part of the endothelium showing fenestra (fs) with its knobbed diaphragm, and two cylindrical channels (ch_1, ch_2). The section grazes the wall of ch_1 and cuts normally through the two diaphragms of ch_2. One of the latter is single-layered, the other is partly triple-layered (arrow). $\times$ 266,000.
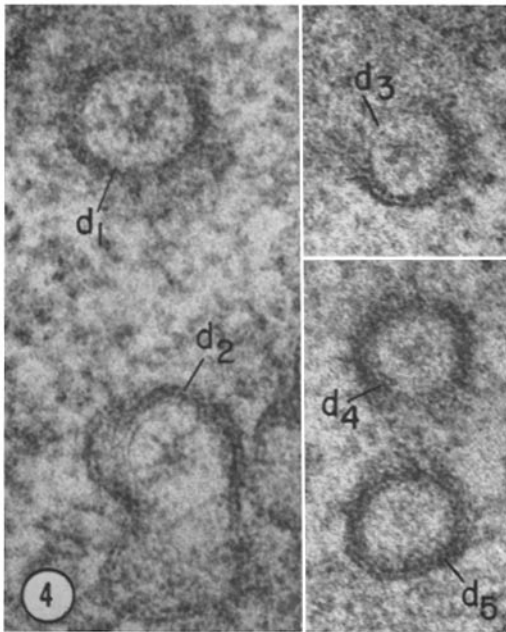

FIGURE 4 Full-face view of a series of five diaphragmed fenestrae (d_1–d_5). The micrographs show that the diaphragms have a central knob (more clearly visible in d_1–d_4), dense streamers radiating from this knob to the fenestral rims (d_1–d_3), and an uneven density in the rest of their areas which varies from very low (d_2) to moderately high (d_4). d_1–d_2, $\times$ 245,000. d_3–d_5, $\times$ 240,000.

gradients between regions facing fenestrae and regions facing thicker parts of the endothelium were no longer apparent. The labeling pattern of plasmalemmal vesicles was not appreciably changed, and the intercellular spaces beyond the junctions contained reaction product at concentrations not higher than the adjacent pericapillary spaces. Some reaction product was also visible in the intercellular spaces of the intestinal epithelium.

5 min after the injection, the concentration of the reaction product in the pericapillary spaces was as high (Fig. 13) or nearly as high (Fig. 14) as in the capillary lumina, suggesting approaching equilibration in enzyme concentration between the plasma and the interstitial fluid. At this time, a large fraction—but not the totality—of the vesicle population of the endothelial cells was marked by reaction product, indifferent of location (interior or fronts of the cells). The situation remained the same between this time and 1 hr after injection. By 24 hr, both the lumen and the pericapillary spaces appeared free of peroxidase.

No concentration gradient of reaction product was detectable on the luminal side or at the level of the basement membrane at any time point. From 2 min on, some reaction product was present, always in small amounts, in the mac-
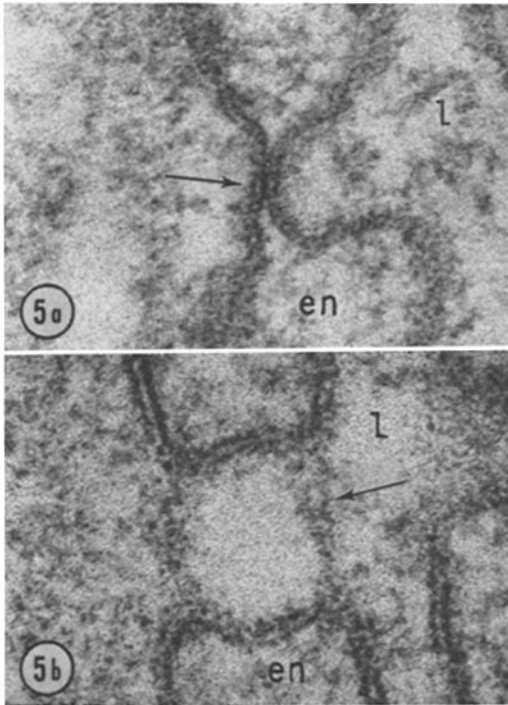
Figure 5 Structural modulations of the endothelium assumed to represent stages in the formation of usual one-layered fenestral diaphragms. *a*, Vesicle opened on the blood front. Its limiting membrane is fused with the plasmalemma on the tissue front to form a five-layered diaphragm (arrow). ×250,000. *b*, Channel closed on the blood front by a diaphragm, part of which has a three-layered structure (arrow). The structure of the diaphragm on the tissue front is obscured by the obliquity of the section. × 370,000.

we carried out the control experiments indicated in Table II. Only rarely did we observe a non-specific reaction in the plasma near red blood cells; it was probably due to hemoglobin leakage by partial hemolysis at the beginning of fixation.

Ferritin Experiments

Tracer molecules were first detected in the pericapillary spaces 3 min after injection, at which time there was a large variation in ferritin permeability among different capillaries: some let pass a substantial amount of tracer, and some apparently none. At 4 min, ferritin was already present in all pericapillary spaces.
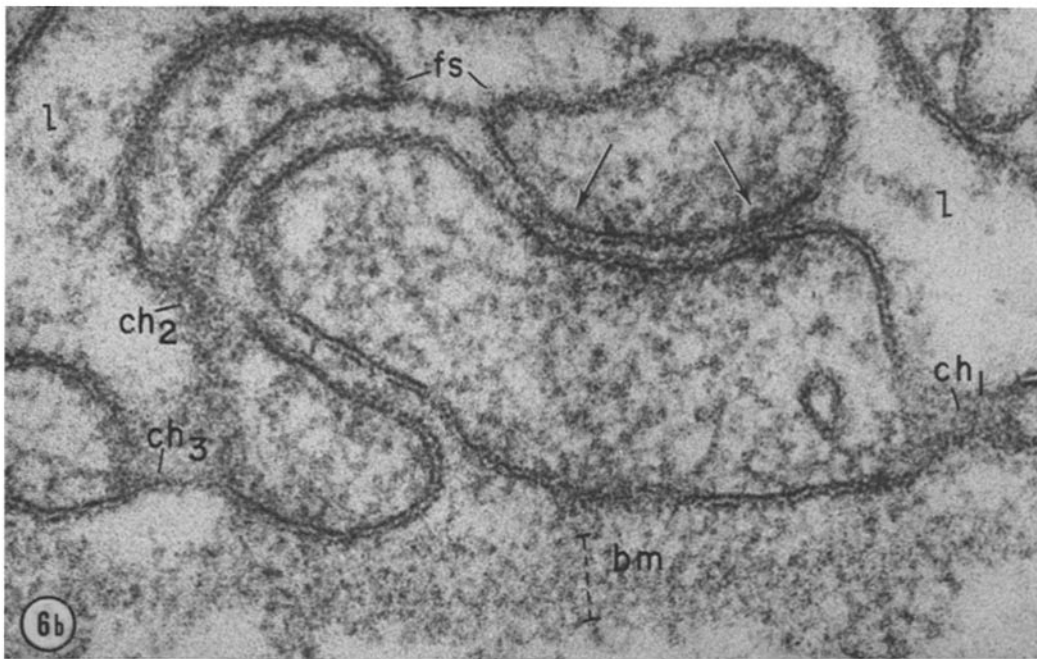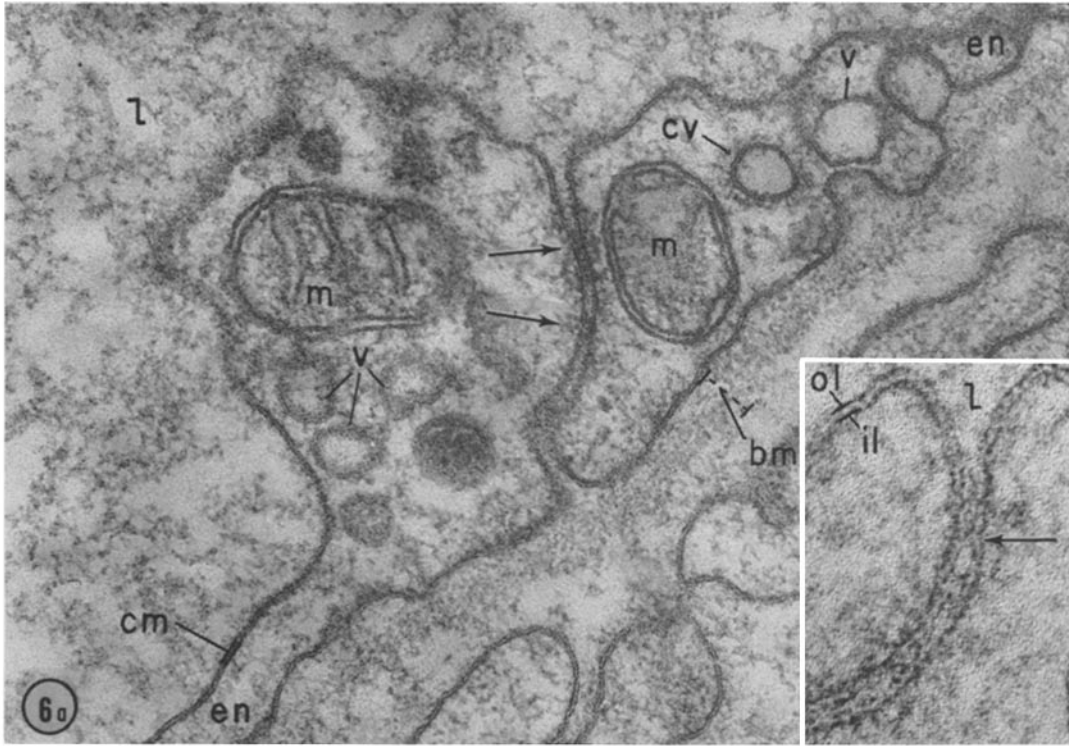
After intravenous injection of 90 mg ferritin[5] in 0.3 ml of saline, the tracer was found evenly distributed in the luminal plasma and remained in high concentration therein for the duration of the 1st hr. Negatively stained preparations of plasma taken at various times after injection revealed no ferritin-ferritin or ferritin-plasma protein aggregates.

From the beginning, tracer molecules appeared to be widely distributed in the pericapillary spaces, but the micrographs suggested that the concentration was higher opposite the fenestrated parts of the endothelium. Ferritin molecules were, hence, counted in the pericapillary spaces in two different types of location: opposite fenestrated (*a*) and nonfenestrated (*b*) parts of the endothelium. The results normalized per μ^2 section are given in Table III. They show first that the concentration of tracer in the pericapillary spaces increased with time and that the ratio a/b de-

rophages of the adventitia and pericapillary spaces (Fig. 15).

To ascertain that the dense material we observed was a specific peroxidase reaction product,

[5] We used this relatively high amount of tracer because smaller doses (30 mg/animal) resulted in too low a concentration of ferritin in the pericapillary spaces for reliable counting.

Figure 6 *a* Junction between two endothelial cells of a blood capillary. The adjacent rims are typically thickened and contain mitochondria and plasmalemmal vesicles, one of which (*cv*) is of coated variety. At a few points along the junction, the apposed cell membranes are either fused or in close contact (arrows). The inset shows an intercellular junction in which the membranes are fused with the focal elimination of the dense outer layers (arrow). × 133,000; inset, × 290,000.

Figure 6 *b* Short-circuited junction between two endothelial cells. The arrows mark limited areas of apparent membrane contact or fusion along this junction. A diaphragmed fenestra (*fs*) opens into the intercellular space behind the junction. Grazing sections along the walls of three channels are marked ch_1–ch_3; ch_2, like fs, opens into the intercellular space behind the junction. × 300,000.

creased from 1.9 at 3 min to 1.12 at 4 min, to 0.77 at 5 min. At all time points investigated, there was a sharp concentration gradient of ferritin at the plasma/endothelium border, irrespective of the structural details of the latter (Fig. 16). Tracer molecules were found lined up along the plasmalemma as well as along the diaphragms of the fenestrae and vesicles (Figs. 17–19) of the endothelial cells, suggesting that the diaphragms generally have a low permeability to ferritin. At 3 and 4 min, most fenestrae appeared impermeable to the tracer (Fig. 17), but occasionally local concentrations or "clouds" of ferritin occurred in the pericapillary spaces opposite an isolated fenestra or a group of fenestrae (Figs. 18, 20, 21). These local concentrations were more striking when located in narrow interstitia, e.g. between endothelial cells and pericytes (Fig. 21). In many cases, the tracer concentration decreased gradually, not abruptly, from the lumen through the fenestra to the pericapillary cloud (Figs. 20 and 21), suggesting that the fenestrae involved were fully permeable to ferritin. The state of the corresponding diaphragms was difficult to ascertain; but we assume that they were partially or entirely missing. Impermeable and permeable fenestrae were found close to one another in sections through the same capillary (Fig. 18), a finding which we take to indicate that permeability to ferritin is a property restricted to certain fenestrae.

The plasmalemmal vesicles of the endothelium were found labeled in all locations from cell front to cell front at, and after 3 min; yet up to 4 min the concentration of the tracer in the adjacent pericapillary spaces remained lower than opposite the fenestrated parts of the endothelium (see Table III).

At all time points examined, ferritin was not found in the intercellular junctions (Fig. 22) and did not accumulate against the basement membrane. From 4 min on, small amounts of tracer molecules were stored in endocytic vacuoles (lysosomes) in the endothelium of blood and lymph capillaries; the uptake was generally more pronounced than in muscle capillaries. Much more ferritin was progressively accumulated within adventitial macrophages in large and numerous vacuoles, which appeared packed with tracer molecules at, and past 1 hr (Fig. 23).

Lymph Experiments

Spectrophotometrically determined concentrations of peroxidase and ferritin in lymph and plasma are given in Figs. 24 and 25. Intravenously injected peroxidase rapidly appeared in the thoracic duct lymph where it reached maximal concentration at 20 min. The concentration ratio lymph/plasma was 0.073 at 20 min and 0.47 at 1 hr. Since the enzyme is rapidly cleared from the plasma by the kidney, a steady-state distribution could not be obtained. The rate of peroxidase appearance in the lymph is comparable to that of albumin (see reference 2).

Intravenously injected ferritin was reduced to half its maximal plasma concentration in ∼7 hr. Its rate of appearance in the thoracic lymph was quite slow; maximal concentration was reached only in ∼4 hr. There was, therefore, a time lag between the appearance of ferritin in pericapillary spaces and its appearance in lymph.

In correlating microscopical findings in the intestinal mucosa with tracer concentrations in the thoracic duct lymph, it should be kept in mind that this lymph represents only in part the interstitial fluid of the intestine, since it is a mix-

Figure 7 Intestinal capillary 1 min 15 sec after an i.v. peroxidase injection. The lumen of the vessel is partially collapsed by a protruding endothelial nucleus in the lower half of the figure. The reaction product fills completely the lumen with a dense homogeneous mass and is present already in the pericapillary spaces that face fenestrated parts of the endothelium (between arrows marked 1). No or little reaction product is detectable in pericapillary spaces facing nonfenestrated endothelium (between arrows marked 2). Note that there is no accumulation of reaction product in the pericapillary spaces opposite the intercellular junctions J (arrows marked 3). Only a few plasmalemmal vesicles marked by reaction product are seen on the tissue front (v_1) of the endothelium, while on the blood front they occur in large numbers (v_2). Note that many plasmalemmal vesicles are still unlabeled (v_3) especially on the tissue side of the perikaryon. An exploded myelin figure, formed at the expense of a mitochondrion, is marked my. × 35,000.
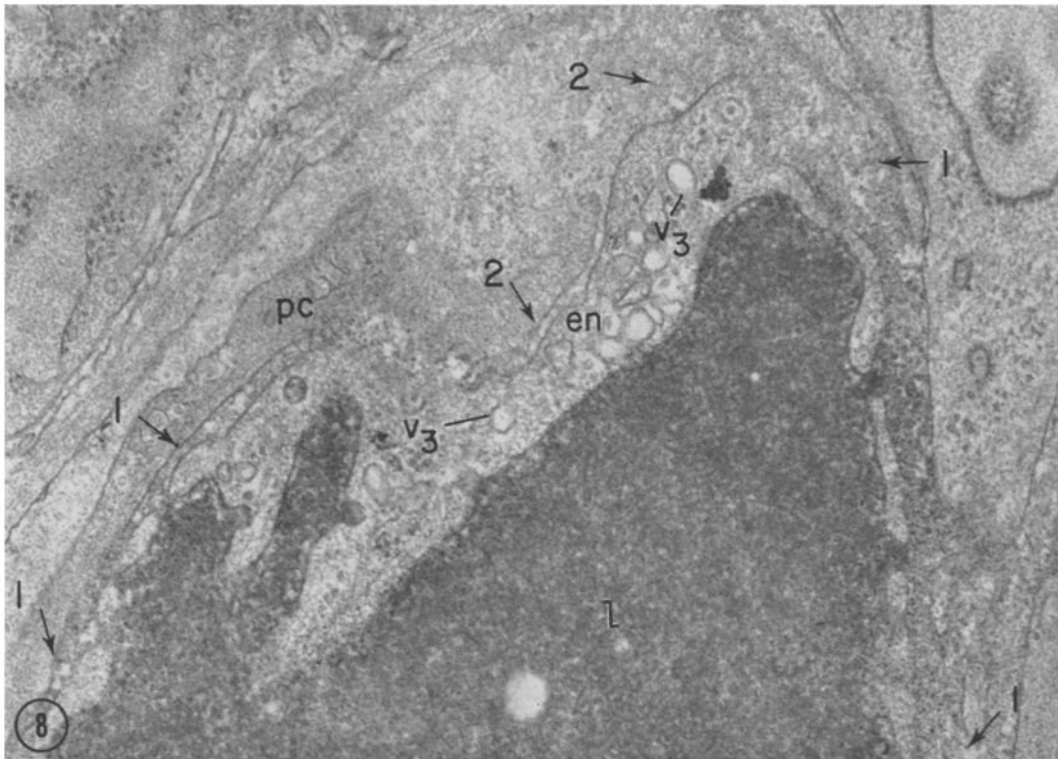
FIGURE 8 Blood capillary 1 min 15 sec after i.v. peroxidase injection. The reaction product in the peri-capillary spaces shows a concentration gradient with two highs opposite fenestrated parts of the endo-thelium (between arrows *1*) and an intercalated low opposite a thicker, nonfenestrated part (between arrows *2*). Note again the limited extent of labeling of the plasmalemma vesicles (v_3). × 42,000.

ture of hepatic, intestinal, and leg lymph. The intestinal component is volumetrically the most important but hepatic lymph, estimated at 10% of the total, has a higher protein concentration. Rates of tracer appearance in the thoracic lymph can represent only maximal figures for the corresponding values in intestinal lymph proper.

The lag observed in the appearance of ferritin in the lymph could be ascribed to macrophage activity, primarily in the intestinal lamina propria, and indicates clearly that equating the chemical composition of capillary filtrate, interstitial fluid, and regional lymph is not fully justified.

DISCUSSION

The basic premises used in the interpretation of our results are the following:

fixation of the probe molecules is fast enough to cope with their diffusion in the intercellular spaces;

the reaction product localizes the peroxidase

within reasonably narrow limits and its concentration is roughly proportional to that of the enzyme.

Peroxidase

On account of its size (diam. ∼50 A), peroxidase is expected to penetrate the small as well as the large pores of the capillary wall. Yet, we can assume that it will mark primarily the former because of their much greater frequency and because molecular sieving effects should not drastically reduce the outflow of an ∼50-A probe through a 90-A pore.[6]

Our results show that peroxidase leaves the lumina of the intestinal capillaries primarily through the diaphragmed fenestrae of the endo-thelium as indicated by the early demonstration

---

[6] As estimated from Grotte's data (1, 3), the outflow of this probe should amount to ∼50% of the outflow of a molecule with a diameter ≤ 10 A.
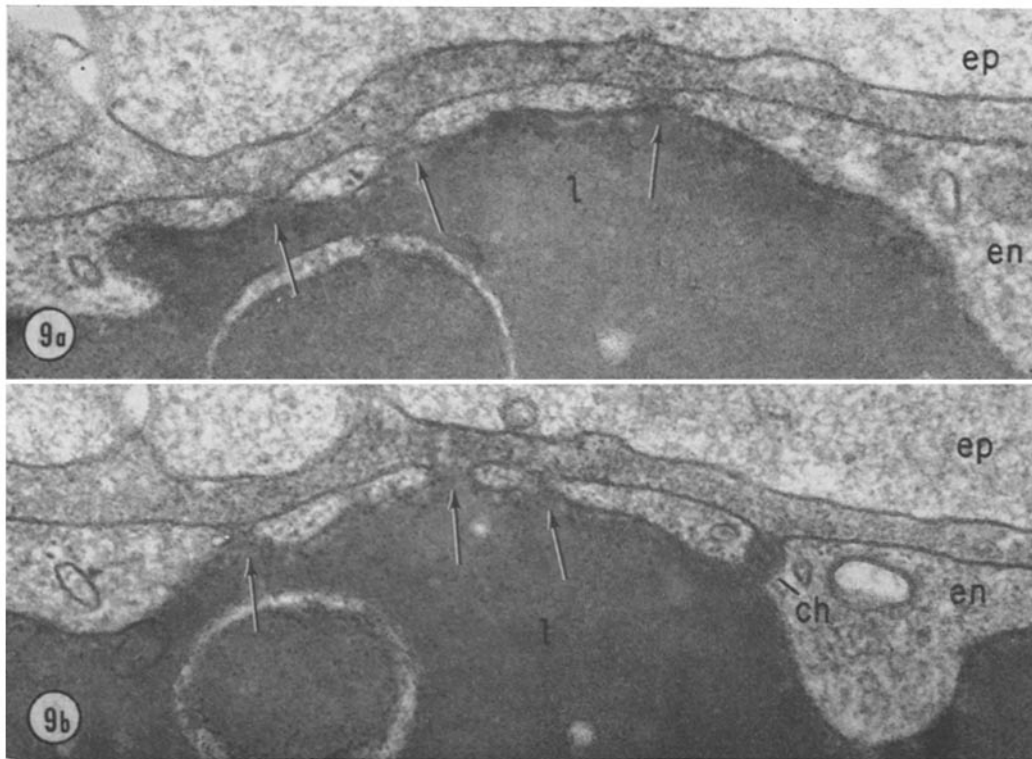
FIGURE 9 *a* and *b* Two serial but nonconsecutive sections through the wall of a blood capillary 1 min 15 sec after an i.v. peroxidase injection. Note that in the pericapillary spaces the reaction product forms a gradient with its maximum opposite the fenestrae (arrows) of the endothelium. The peroxidase-labeled structure at *ch* is probably a newly formed cylindrical channel opened on both fronts of the endothelium. × 105,000.

of concentration gradients of reaction product in the pericapillary spaces, high opposite fenestrated areas of the endothelium and low elsewhere, as well as by the demonstration of local concentrations of such product opposite isolated individual fenestrae. The evidence suggests that peroxidase is also transported by plasmalemmal vesicles since enzyme-labeled vesicles were found in all expected endothelial locations, and since discharging vesicles were seen on the tissue front of the endothelium. The results indicate, however, that these vesicles do not represent the main pathway followed by the tracer and that their movement is slow since a fraction of the vesicle population remained unlabeled by peroxidase at a time (5–10 min) when the tracer reached a uniform, relatively high concentration in the pericapillary spaces.

One to 1.5 min after i.v. peroxidase injection, the

intercellular spaces of the endothelium remained free of reaction product beyond their junctional elements and later on (up to 5 min), concentration within these spaces was lower or at most equal to that found in the pericapillary spaces. At no time point could we detect concentration gradients in the pericapillary spaces with their highs opposite the intercellular junctions of the endothelium. In view of the inherent limitations of the procedure, movement of peroxidase molecules through intercellular junctions could not be ruled out entirely, but it appeared to be negligible by comparison with its movement through diaphragmed fenestrae.

Ferritin

The experiments with ferritin—used as a probe molecule for the large pore system—gave partly similar results. Early and transient con-
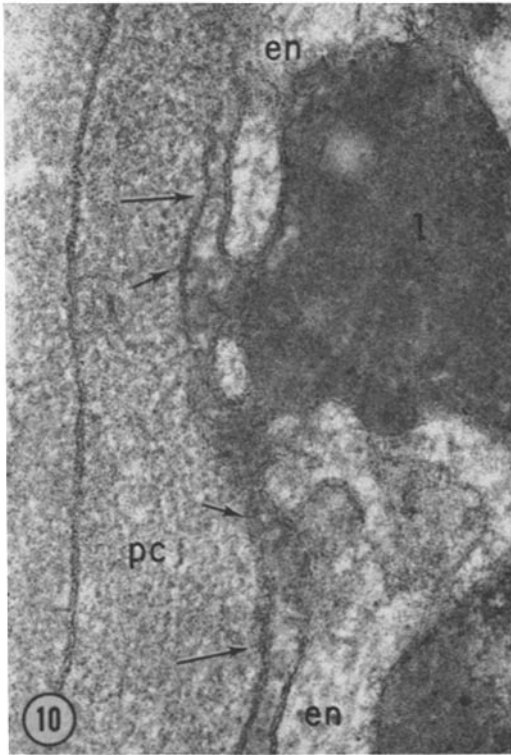
FIGURE 10   Blood capillary 1 min 15 sec after an i.v. peroxidase injection. The field shows two fenestrae opening into a narrow space between an endothelial cell and a pericyte (pc). Note the high concentration of reaction product in the lumen and the nearly as high concentration in the subendothelial space opposite the two fenestrae (short arrows). In this space the concentration drops rapidly above and below the fenestrated area (long arrows) thus forming a sharp gradient with its high opposite the fenestrae. × 145,000.

centration gradients were found in the pericapillary spaces with highs opposite the fenestrated regions of the endothelium, although these gradients were less obvious than in the case of peroxidase. There was only suggestive evidence for concomitant vesicular transport, and there was no evidence for the movement of the ferritin through intercellular junctions. In both cases, at early time points, there was only one steep concentration gradient at the plasma/endothelium interface, and there was no accumulation of tracers against the basement membrane, or any other structural element of the capillary wall.

Taken together, these results strongly suggest that in the blood capillaries of the mouse intestine

the small as well as the large pore system is located in the fenestrated part of the endothelium, most probably in the diaphragms of its fenestrae. The morphology of these structures was debated for some time (see references 8, 12), but recently Luft on intestinal capillaries (10, 29) and Elfvin on the vessels of the adrenal medulla (30) have firmly established that the diaphragms of the endothelial fenestrae have no unit membrane structure and consist, instead, of a single dense layer continuous with the outer dense leaflet of the plasmalemma.

According to current interpretations, the absence of stratified structure, especially the absence of an intermediate light layer, implies that the diaphragms consist primarily of a protein-polysaccharide film and do not have a continuous (or quasi-continuous) hydrophobic phase. The permeability of such a structure is expected to be much higher than that of a usually constructed cell membrane. Hence, a priori, pore localization at the level of the diaphragms is to be anticipated. Yet full agreement with the pore theory of capillary permeability requires the demonstration of: (a) diaphragm openings of ∼90 A diameter and relatively high frequency $(15–20/\mu^2)$, for the small pore system; and (b) a small number (less than 0.3% of the total population) of nonapertured fenestrae, for the large pore system, since the diameter of a fully opened fenestra (350–450 A) approaches that postulated for a large pore (∼500 A). Both points are difficult, if not impossible, to establish by current electron microscopical procedures. There is at present no reliable evidence on discontinuities in fenestral diaphragms,[7] and a major operation of uncertain results would be required to establish the existence of a fully opened fenestra per ∼17 μ^2 (or more) of endothelial surface. Our findings indicate, however, that the sites of ferritin exit must be much more frequent in space than the large pores are assumed to be. With exit restricted over a long period of time to one fenestra/17 μ^2 (or more) of endothelial surface, ferritin concentration gradients in the pericapillary spaces should be much rarer, sharper, and more lasting than they were found to be in our experiments. A plausible explanation for this discrepancy is that the dia-

[7] The postulated localization of an ∼90 A diameter pore to the middle of the central knob (29) is highly questionable.
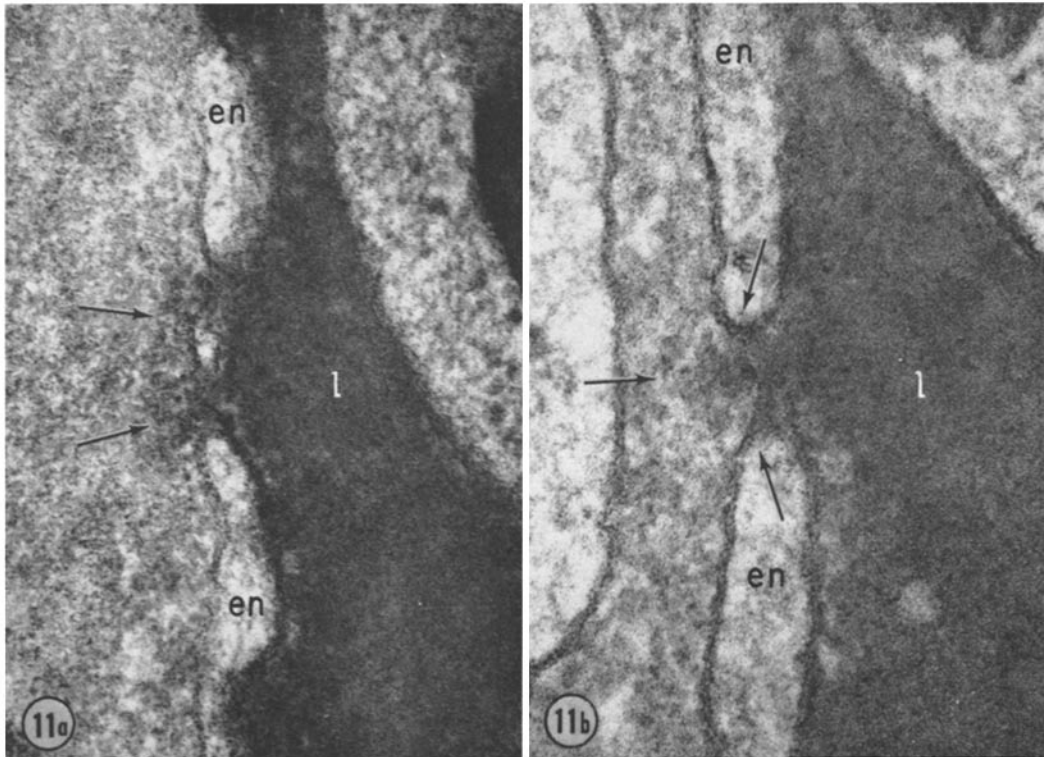
FIGURE 11   Blood capillary 1 min 15 sec after an i.v. peroxidase injection. Focal concentrations of reaction product (long arrows) appear in the pericapillary spaces directly opposite two fenestrae in Fig. 11 a and a fenestra in Fig. 11 b. In the latter, the presence of a diaphragm and its position can be made out: the lower and upper arrow point to its insertion into the fenestral rim. a, × 160,000. b, × 190,000.
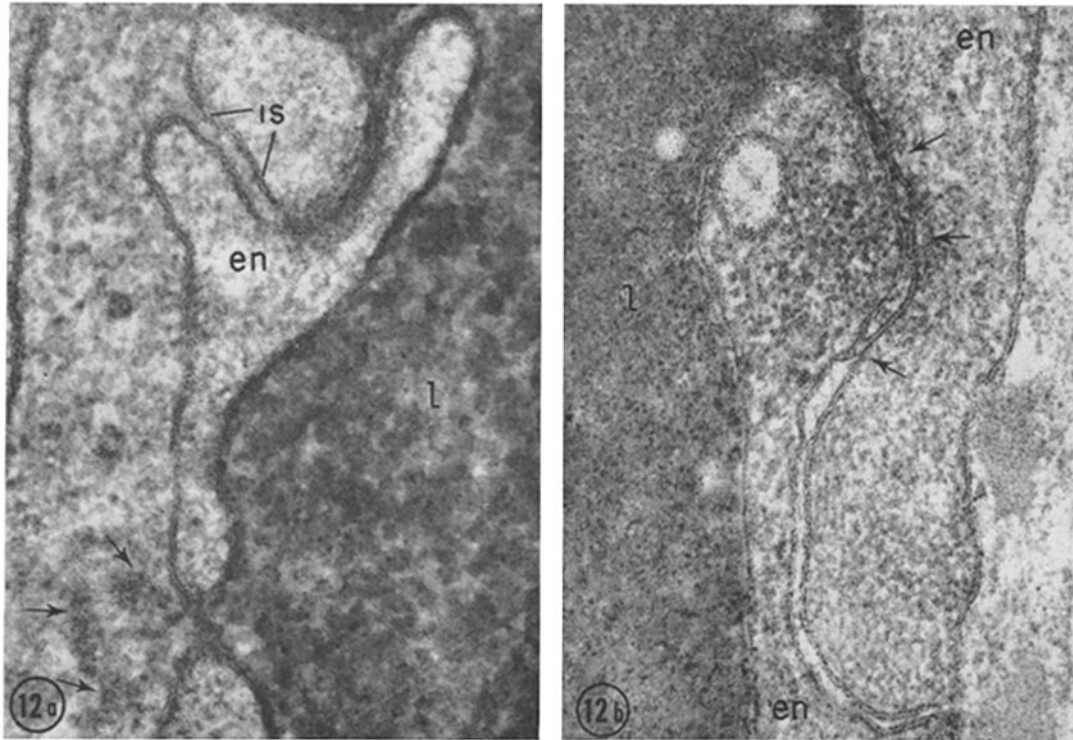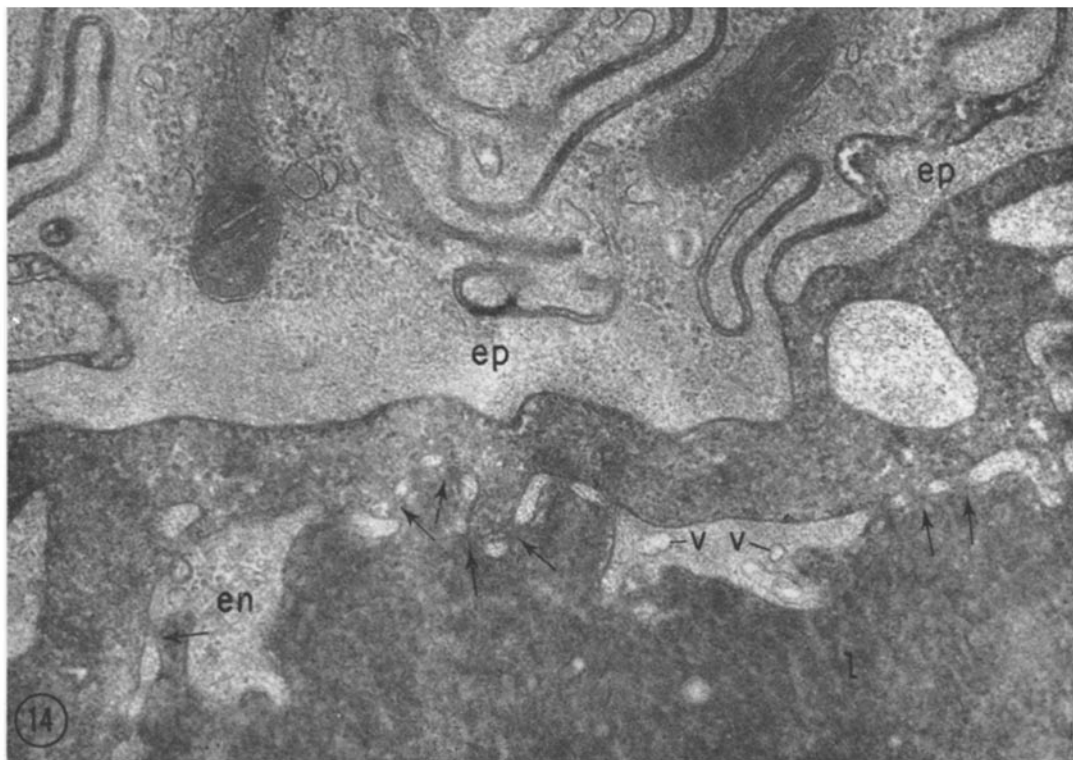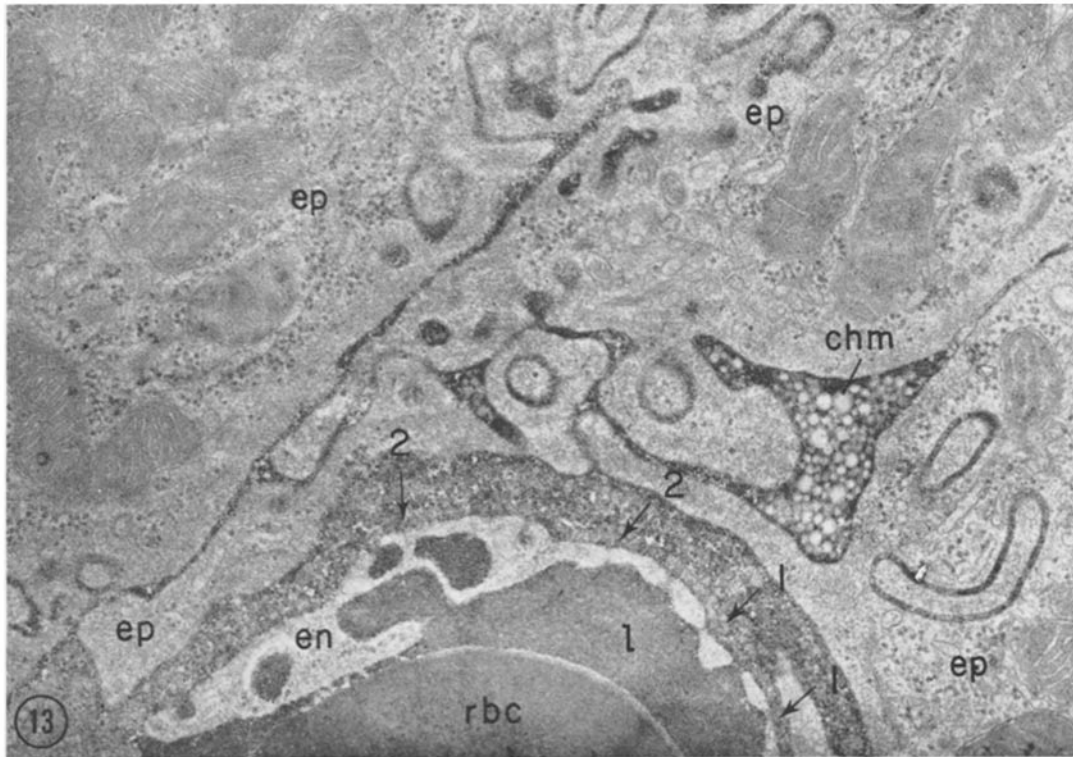
FIGURE 12   Intercellular junctions of the endothelium of peroxidase-labeled capillaries. a, Capillary 1 min 45 sec after an i.v. peroxidase injection. A localized cloud of reaction product (arrows) is seen in the pericapillary spaces directly opposite a fenestra. The condition of the fenestral diaphragm can not be ascertained, for its structure is obscured by the peroxidase reaction product. A neighboring intercellular space (is) is occupied only half-way by the reaction product, presumably up to a tight junction; the abluminal end and the adjacent pericapillary space is free of it. At this magnification, the reaction product filling the lumen appears less homogeneous and is partly resolved in lumps of ∼200 A. × 120,000.

b, Capillary 1 min after an i.v. injection of peroxidase. Three successive areas of intercellular membrane contact or fusion are marked by arrows. The reaction product fills the intercellular space from the lumen as far as the last junctional element which appears to be an occluding zonule; its concentration drops, however, sharply after the first element. × 125,000.

Figures 13 and 14   Mouse intestine 10 min after an i.v. injection of peroxidase. In Fig. 13, the pericapillary spaces are completely and evenly filled with dense reaction product, which is also present in the intercellular spaces of the intestinal epithelium (note that chilomicra (chm) appear in negative contrast in these spaces). The intensity of the reaction in the vascular lumen is still higher than in the pericapillary spaces but gradients can no longer be observed in the pericapillary spaces between regions opposite fenestrated (arrows 1) and nonfenestrated (arrows 2) parts of the endothelium. × 24,000.

In Fig. 14, the situation is similar to the one in Fig. 13, except that the intensity of the reaction in the pericapillary spaces is nearly as high as in the capillary lumen. Because of the heavy accumulation of reaction product, neither the basement membrane, nor elements of the adventitia are visible. Only the endothelial tunic is clearly recognizable. Some of its fenestrae are marked by arrows. Note that some of the plasmalemmal vesicles (v) of the endothelium are still unlabeled. Note also the occurrence of reaction product in the intercellular spaces of the epithelium. × 48,000.
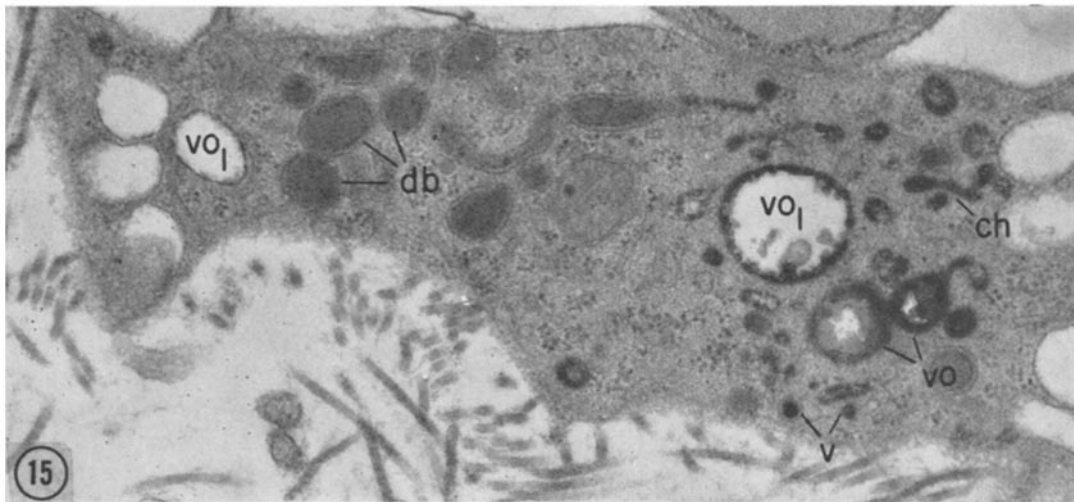
FIGURE 15 Mouse intestinal mucosa 15 min after an i.v. injection of peroxidase. The micrograph shows a macrophage in the adventitia of a blood capillary. A number of endocytic structures in this cell contain peroxidase reaction product which appears to be more concentrated in small vesicles (v) and channels (ch) than in large vacuoles (vo). Some of the latter have only an inner coating of reaction product (vo_1). The group of dense bodies marked db is peroxidase-negative; its formation presumably preceded the exposure to peroxidase. $\times$ 31,000.

TABLE II

Control Experiments to Evaluate the Specificity of Peroxidase Reaction with 3–3′ Diaminobenzidine

| .v. Injection | Reagents present in the incubation medium | | | Reaction |
	Substrate	H₂O₂	Peroxidase	
Peroxidase	Present	Present	No	+
Peroxidase	Present	No	No	−
Peroxidase	No	Present	No	−
Saline	Present	Present	No	−
Saline	Present	Present	Present	−

TABLE III

Ferritin Concentration in Capillary Lumina and Pericapillary Spaces

| Time after injection | Molecules/μ² section* | | | |
	Lumen	A	B	A/B
min				
3	2780	44.4	23.1	1.9
4	2050	119	105	1.12
5	1640	112	140	0.77

* Areas were measured on micrographs with a Keuffel and Esser planimeter. Twenty-three different micrographs were used for each time point.

A = pericapillary region opposite fenestrated endothelium.

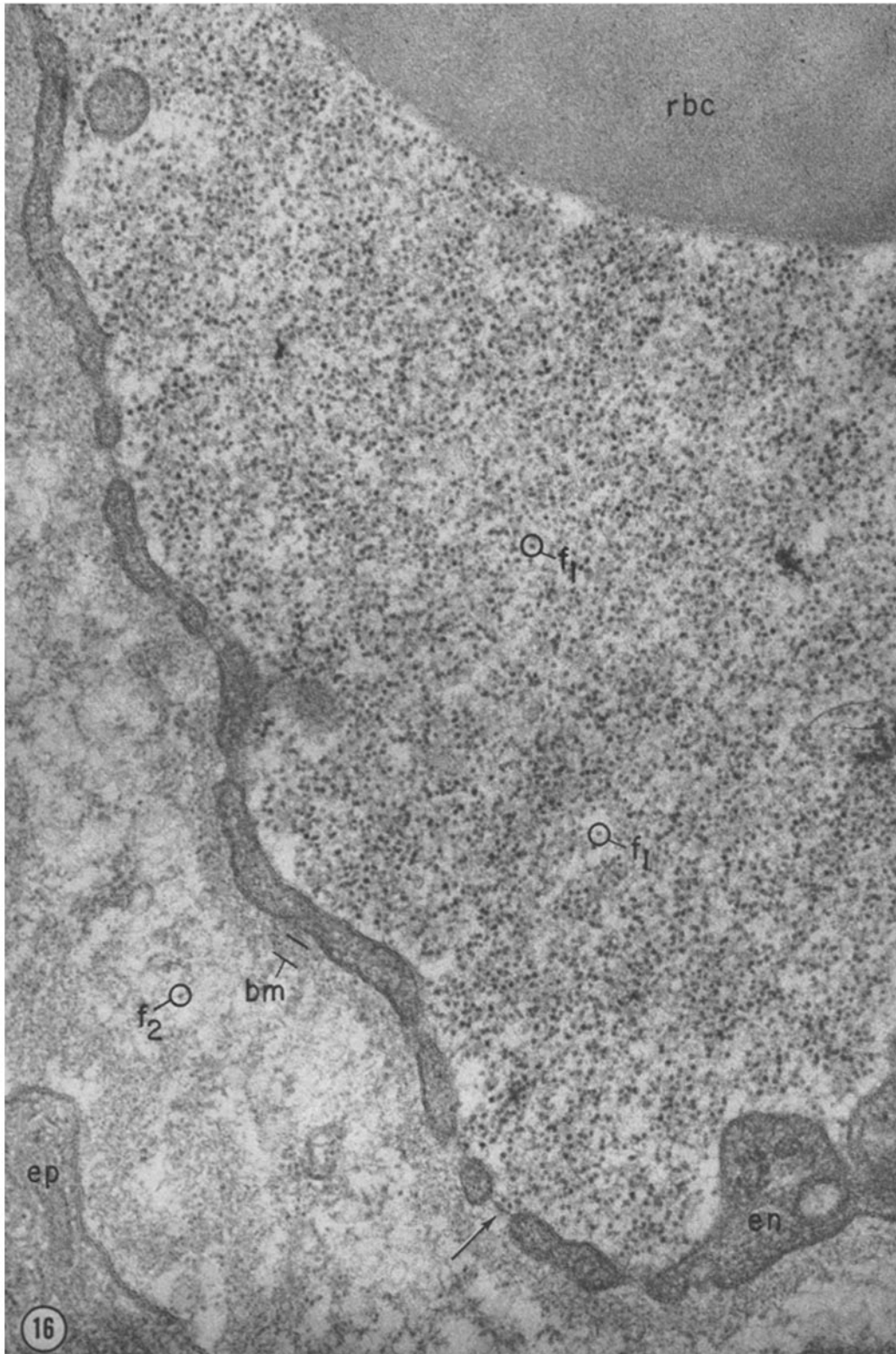B = pericapillary region opposite non-fenestrated endothelium.

The aggregate areas over which ferritin molecules were counted were:

3 min: A, 8.76 μ² (389) ; B, 17.69 μ² (410)

4 min: A, 9.76 μ² (1167) ; B, 18.23 μ² (1929).

Total number of molecules in each aggregate area is given in brackets.

phragms are unstable structures in which transient discontinuities of the required dimensions can develop in different locations at such a rate as to insure at any time the frequency postulated by the pore theory. Preliminary experiments indicate that diaphragms depend for their existence on local Ca^{2+} concentration (F. Clementi and G. E. Palade. Unpublished observations).

Since the large pore system has been connected with the plasmalemmal vesicles in muscle capillaries (6), the relationship of diaphragmed fenes-

trae to such vesicles requires further comments. Recently, Palade and Bruns (26) have presented evidence which suggests that—irrespective of their location—i.e., within fenestrae or stomata of

FIGURES 16–22   Blood capillaries of the intestinal mucosa 4 min after an i.v. injection of ferritin.

FIGURE 16   Fenestrated part of a capillary facing the intestinal epithelium. Ferritin is present in high concentration and relatively even distribution in the plasma (f_1); very few molecules have reached the pericapillary spaces (f_2). This sharp concentration gradient is maintained along the entire endothelial sector, irrespective of its fenestrations. The arrow points out an impermeable fenestral diaphragm. $\times$ 100,000.

FIGURE 17   shows four endothelial fenestrae, one (fs_1) obliquely, and the other three (fs_2–fs_4) normally sectioned. The tracer fills the lumen and the channels leading to the fenestrae, but does not penetrate beyond the expected level of the fenestral apertures in fs_2–fs_4. The apertures themselves are not clearly visible. In this case, no ferritin has yet reached the pericapillary spaces. × 100,000.
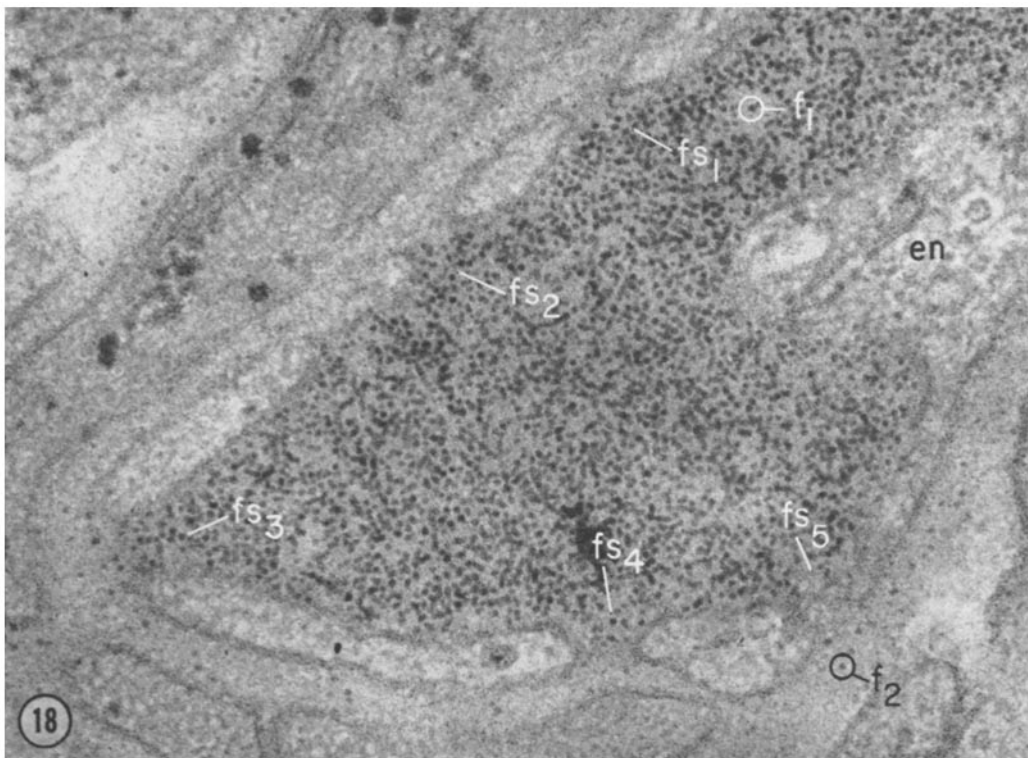

FIGURE 18   shows five endothelial fenestrae of which two (fs_1, fs_2) are not penetrated by ferritin. The tracer appears to move freely out of the lumen through fs_3 as suggested by the cloud of molecules opposite this fenestra. fs_4 and fs_5 may also be permeable since ferritin molecules are present in the pericapillary space in their immediate vicinity. In their case, however, there is a sharp gradient of ferritin concentration at the level of the fenestral apertures and no well defined tracer clouds in the pericapillary space opposite the fenestrae. × 115,000.
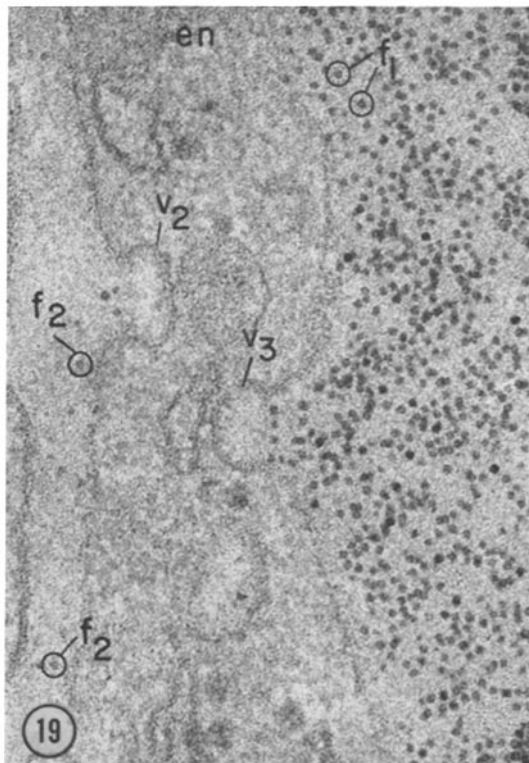
52

FIGURE 19 Four ferritin molecules appear aligned on the diaphragm of a vesicle (v_3) that has a tracer-free content and is apparently ready to open on the blood front. Such appearances suggest that the diaphragms limit—to a certain extent—the diffusion of ferritin. The vesicle marked v_2 has apparently discharged three ferritin molecules on the tissue front of the endothelium. × 240,000.
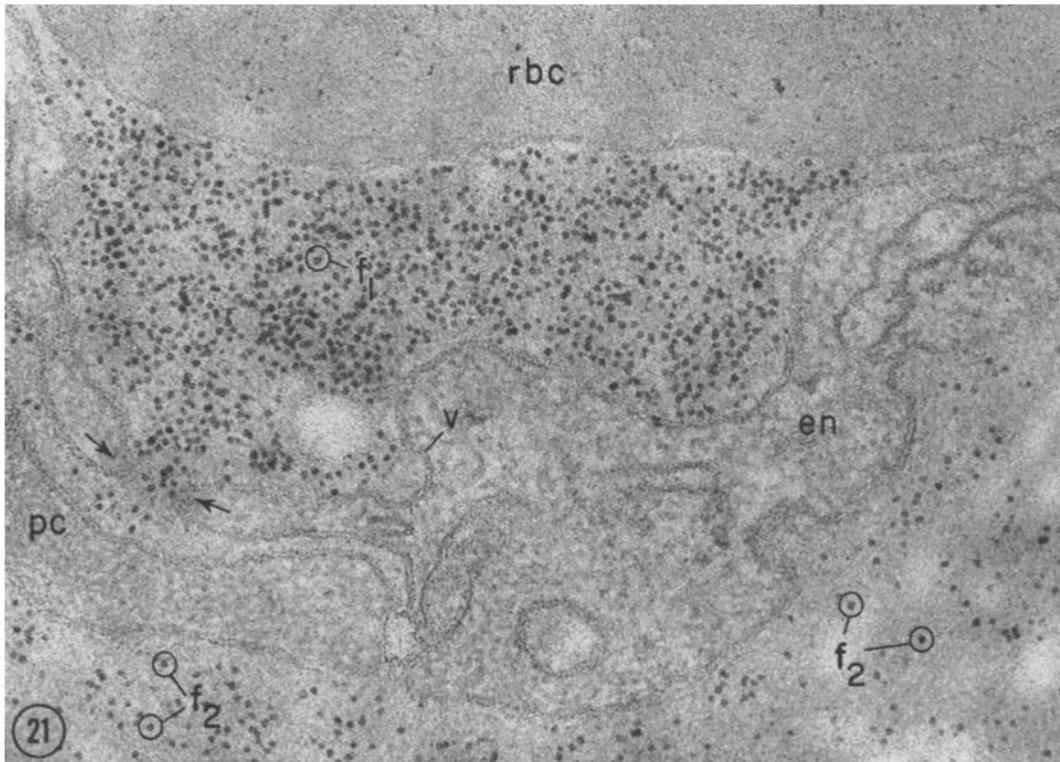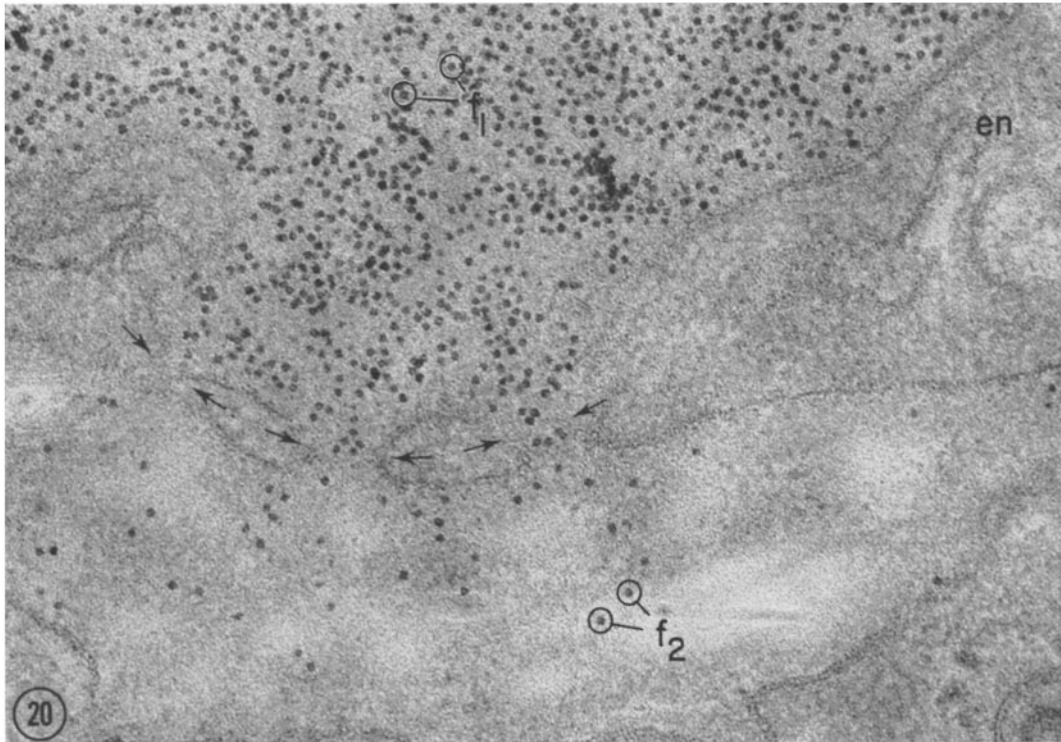
vesicles—diaphragms are the result of the fusion of two membranes followed by a progressive elimination of their layers.[8] In the case of diaphragmed vesicles, one membrane is the plasmalemma, the other the limiting membrane of the vesicle. The same seems to apply in the case of doubly apertured channels, except that the process affects concomitantly the membrane of the same vesicle and the plasmalemma on both fronts of the cell. A singly apertured fenestra may derive from such a channel upon the loss of one of its two diaphragms, or may be produced by direct fusion of the plasmalemma on the blood front to that on the tissue front of the cell. In any case, exchanges between the two compartments separated by a diaphragm would be controlled by the latter's permeability.

Bruns and Palade (6, 26) have discussed the

difficulties encountered in bringing into agreement morphological findings and physiological data on muscle capillary permeability. They have pointed out that general agreement could be reached by assuming that in vivo plasmalemmal vesicles form continuous channels from cell front to cell front, and that these channels occur with the frequency required by the pore theory and are provided with a constriction of appropriate effective diameter (∼90 A or 500 A) located either in between vesicles or in the stomatic diaphragm of a discharging vesicle. The situation found in the capillaries of the intestinal mucosa is, in fact, a variant of this postulate. The arrangement probably survives preparation procedures, because the number of vesicles in a connecting chain is generally reduced to one or maximum two.

The identification of the apertured fenestrae as the site of the small pore system in intestinal capillaries appears reasonably well established. The evidence as to the other possible location, i.e., the intercellular junctions (see reference 7) has been consistently negative, and the possibility

[8] The formation of pores (31) and the opening of vesicles (32) by membrane fusion has also been postulated by Wolff and Merker. In their interpretation, the single-layered diaphragm, however, is not a residue of the strata of the fused membranes, but an extraneous film of adsorbed plasma proteins.

FIGURES 20 and 21   The micrographs demonstrate high, focal concentrations of ferritin which appear opposite individual fenestrae (arrows) and are located in the basement membrane and pericapillary spaces (or intercellular space between an endothelial cell and a pericyte in Fig. 21). The conditions of the corresponding diaphragms cannot be ascertained. An apertured vesicle not penetrated by ferritin appears at v on the blood front of the endothelium in Fig. 21. Fig. 20, $\times$ 165,000. Fig. 21, $\times$ 180,000.
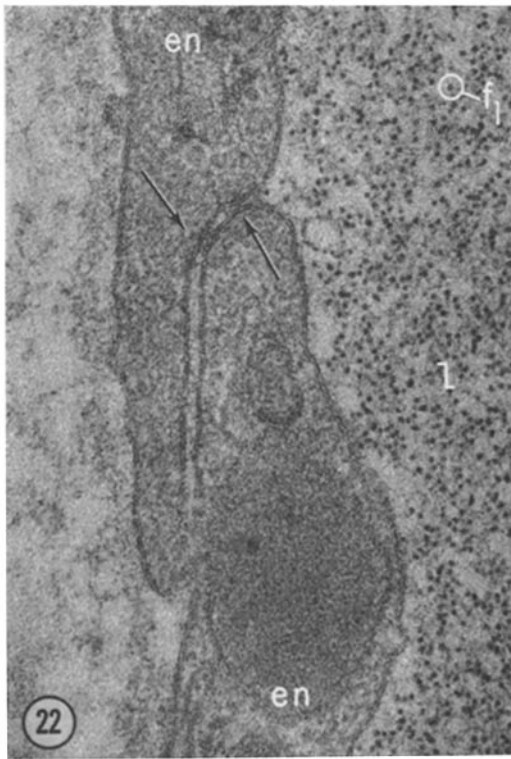
that the fenestrae represent the large rather than the small pore system can be ruled out with enough confidence. Peroxidase penetrates both pore systems; hence its passage through the fenestrae is necessary but not sufficient to identify these structures as the sites of the small pores. Yet were the fenestrae the large pores and were they opened to a diameter of ~500 A, as required by the pore theory, their aggregate area would amount to ~10% of the total capillary surface. With such extensive coarse porosity, the capillary would retain practically no restricted permeability to large molecules, which is contrary to established facts (2, 3). Even for the leakiest capillary known, the liver sinusoid, the pore theory does not require an aggregate large pore area greater than 0.01% of the total surface of the vessel.

Recently Alvarez and Yudilevich, working on the stomach (33) and heart (34) of the dog, have found that the outflow of $^{22}Na^+$ from the plasma is more restricted than that of tritiated water. They could not explain their findings by assuming that the same fractional area of capillary surface is available for both outflows (as assumed in the pore theory) and postulated that $^{22}Na^+$ moves

only through the intercellular spaces while HTO exchanges through these spaces as well as through the cells of the endothelium. At least in the case of the stomach, these findings suggest a certain degree of heteroporosity within fenestral diaphragms.

The identification of large pores with permanently or temporarily patent fenestrae is less certain. It can be questioned on account of the evidence obtained with graded dextrans by Meyerson et al. (2). As already mentioned, this evidence suggests that the small pores of intestinal capillaries have diameters of ~220 A, which would make them permeable to ferritin. Under these circumstances, the identification we have proposed should be considered tentative and should be checked in future experiments by the use of probes with a larger molecular diameter (250–500 A) than ferritin.
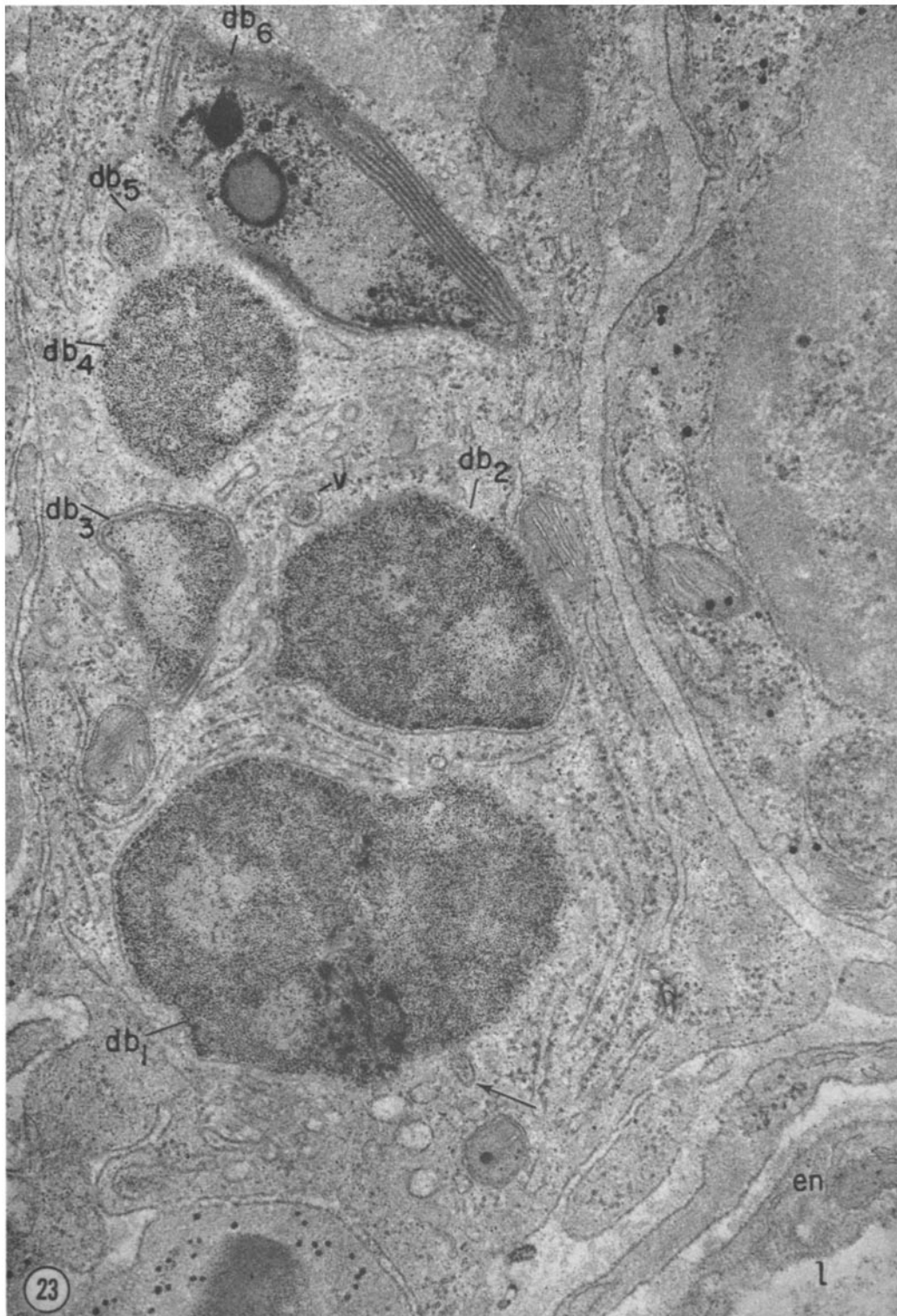
FIGURE 23   Macrophage in the vicinity of a blood capillary (lower right corner) 60 min after an i.v. ferritin injection. Tracer molecules are present in high, uneven concentration in six dense bodies (db_1–db_6) wherein they occur mixed with a variety of residues of previous phagocytic activity. In addition, the tracer is found in small vacuoles (v) and vesicles, one of which is apparently fusing (arrow) with db_1. Ferritin molecules, presumably of endogenous origin, are present in relatively high concentration in the cytoplasmic matrix of the macrophage. × 34,000.

Horseradish Peroxidase Concn in Plasma and Lymph

○ Plasma
● Lymph

μg/ml

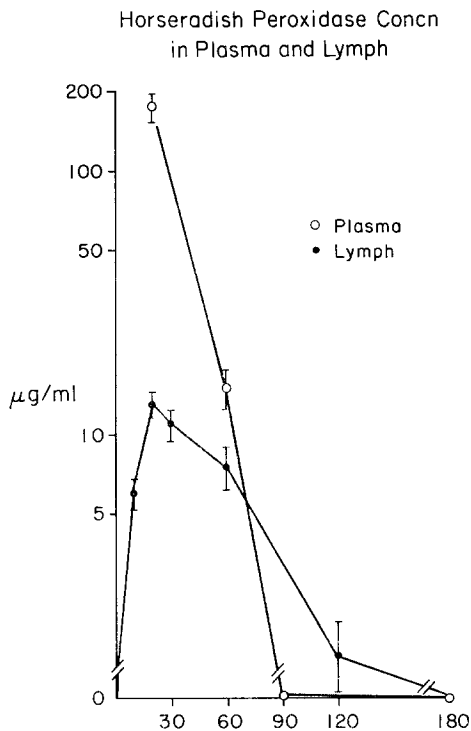**Ferritin Concentration in Plasma and Lymph**

μg/ml

○ Plasma
● Lymph

Hours

FIGURE 24 Peroxidase concentration in lymph and plasma as a function of time after an i.v. injection. Each point is the mean ± standard error of four determinations. The mean lymph flow during the experiments was 0.62 ml/hr. The L/P ratios were 0.073 ± 0.011 at 20 min and 0.47 ± 0.13 at 1 hr.
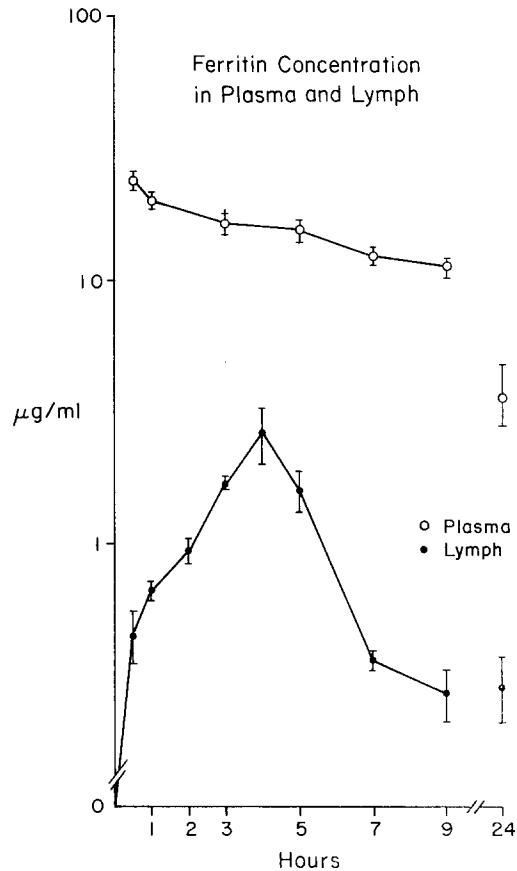
FIGURE 25 Ferritin concentration in lymph and plasma as a function of time after an i.v. injection. Each time point is the mean ± standard error of five determinations. The mean lymph flow during the experiments was 0.4 ml/hr. The L/P ratios were: 0.018 ± 0.004 at 30 min; 0.034 ± 0.0037 at 1 hr; 0.093 ± 0.009 at 3 hr; 0.094 ± 0.026 at 5 hr; 0.028 ± 0.0036 at 7 hr; 0.023 ± 0.0053 at 9 hr; and 0.094 ± 0.032 at 24 hr.

REFERENCES

1. GROTTE, G., 1956. Passage of dextran molecules across the blood-lymph barrier. Acta Chir. Scand. Suppl. 211:1.
2. MAYERSON, H. S., C. G. WOLFRAM, H. H. SHIRLEY, JR., and K. WASSERMAN. 1960. Regional differences in capillary permeability. Amer. J. Physiol. 198:155.
3. LANDIS, E. M., and J. R. PAPPENHEIMER. 1963. Exchange of substances through the capillary walls. In Handbook of Physiology. Section 2, Circulation Vol. II. W. F. Hamilton and P. Dow, editors. American Physiology Society, Washington, D. C.

4. RENKIN, E. M. 1964. Transport of large molecules across capillary walls. Physiologist. 7:13.
5. BENNETT, H. S., L. H. LUFT, and J. C. HAMPTON. 1959. Morphological classification of vertebrate blood capillaries. Amer. J. Physiol. 196: 381.
6. BRUNS, R. R., and G. E. PALADE. 1968. Studies on blood capillaries. II. Transport of ferritin molecules across the wall of muscle capillaries. J. Cell Biol. 37:277.
7. KARNOVSKY, M. J. 1967. The ultrastructural basis of capillary permeability studies with peroxidase as a tracer. J. Cell Biol. 35:213.

8. Rhodin, J. A. G. 1962. The diaphragm of capillary endothelial fenestrations. *J. Ultrastruct. Res.* **6:**171.

9. Fawcett, D. W. 1963. Comparative observations on the fine structure of blood capillaries. *In* The Peripheral Blood Vessels. *Int. Acad. Pathol. Monogr. No. 4.*, O. L. Orbison and D. E. Smith, editors. Baltimore. p. 17.

10. Luft, J. H. 1965. The ultrastructural basis of capillary permeability. *In* The Inflammatory Processes. Academic Press Inc., New York. p. 121.

11. Farquhar, M. G. 1961. Fine structure and function in capillaries of the anterior pituitary gland. *Angiology.* **12:**270.

12. Karrer, H. E., and J. Cox. 1960. The striated musculature of blood vessels. II. Cell interconnections and cell surface. *J. Biophys. Biochem. Cytol.* **8:**135.

13. Farquhar, M. G., and G. E. Palade. 1961. Glomerular permeability. II. Ferritin transfer across the glomerular capillary wall in nephrotic rats. *J. Exp. Med.* **114:**699.

14. Karnovsky, M. J. 1965. A formaldehyde-glutaraldehyde fixative of high osmolarity for use in electron microscopy. *J. Cell Biol.* **27:**137A. (Abstr.)

15. Smith, R. E., and M. G. Farquhar. 1963. Preparation of thick sections for cytochemistry and electron microscopy by a non freezing technique. *Nature.* **200:**691.

16. Graham, R. C., and M. J. Karnovsky. 1966. The early stages of absorption of injected horseradish peroxidase in the proximal tubules of mouse kidney. Ultrastructural cytochemistry by a new technique. *J. Histochem. Cytochem.* **14:**291.

17. Farquhar, M. G., and G. E. Palade. 1965. Cell junctions in amphibian skin. *J. Cell Biol.* **26:**263.

18. Luft, G. H. 1961. Improvements in epoxy embedding methods. *J. Biophys. Biochem. Cytol.* **9:**409.

19. Venable, J., and R. Coggeshall. 1965. A simplified lead citrate stain for use in electron microscopy. *J. Cell Biol.* **25:**407.

20. Boak, J. L., and M. F. A. Woodruff. 1965. A modified technique for collecting mouse thoracic duct lymph. *Nature.* **205:**396.

21. Morse, S. I., and S. K. Riester. 1967. Studies on the leucocytosis and lymphocytosis induced by Bordetella pertussis. II. The effect of pertussis vaccine on the thoracic duct lymph and lymphocytes of mice. *J. Exp. Med.* **125:** 619.

22. Straus, W. 1958. Colorimetric analysis with N,N-dimethyl-p-phenylenediamine of the uptake of intravenously injected horseradish peroxidase by various tissues of the rat. *J. Biophys. Biochem. Cytol.* **4:**541.

23. Delaney, J. P., and E. Grim. 1964. Canine gastric blood flow and its distribution. *Amer. J. Physiol.* **207:**1195.

24. Weibel, E. R., and G. E. Palade. 1964. New cytoplasmic components in arterial endothelium. *J. Cell Biol.* **23:**101.

25. Fuchs, A., and E. R. Weibel. 1966. Morphometrische Untersuchung der Verteilung einer spezifischen cytoplasmatische Organelle in Endothelzellen der Ratte. *Z. Zellforsch.* **73:**1.

26. Palade, G. E., and R. R. Bruns. 1968. Structural modulation of plasmalemmal vesicles. *J. Cell Biol.* **37:**633.

27. Bruns, R. R., and G. E. Palade. 1968. Studies on blood capillaries. I. General organization of muscle capillaries. *J. Cell Biol.* **37:**244.

28. Greenlee, T. K., Jr., R. Ross, and J. L. Hartman. 1967. The fine structure of elastic fibers. *J. Cell Biol.* **30:**59.

29. Luft, J. H. 1964. Fine structure of the diaphragm across capillary "pores" in mouse intestine. *Anat. Rec.* **148:**307.

30. Elfvin, L. G. 1965. The ultrastructure of the capillary fenestrae in the adrenal medulla of the rat. *J. Ultrastruct. Res.* **12:**687.

31. Wolff, J., and H. J. Merker. 1966. Ultrastruktur und Bildung von Poren in Endothel von porösen und geschlossenen Kapillaren. *Z. Zellforsch.* **73:**174.

32. Wolff, J. 1966. Elektronenmikroskopische Untersuchungen über die Vesikulation in Kapillarenendothel. Lokalisation, Variation, und Fusion der Vesikel. *Z. Zellforsch.* **73:**143.

33. Alvarez, O. A., and D. L. Yudilevich. 1967. Capillary permeability and tissue exchange of water and electrolytes in the stomach. *Amer. J. Physiol.* **213:**315.

34. Yudilevich, D. L., and O. A. Alvarez. 1967. Water, sodium, and thiourea transcapillary diffusion in the dog heart. *Amer. J. Physiol.* **213:**308.